Anomalous velocity distributions in inelastic Maxwell gases

R. Brito M. H. Ernst

Published in: ”Advances in Condensed Matter and Statistical Physics”, E. Korutcheva and R. Cuerno (eds.), Nova Science Publishers, New York (2004), pp. 177–202.

This review is a kinetic theory study investigating the effects of inelasticity on the structure of the non-equilibrium states, in particular on the behavior of the velocity distribution in the high energy tails. Starting point is the nonlinear Boltzmann equation for spatially homogeneous systems, which supposedly describes the behavior of the velocity distribution function in dissipative systems as long as the system remains in the homogeneous cooling state, i.e. on relatively short time scales before the clustering and similar instabilities start to create spatial inhomogeneities. This is done for the two most common models for dissipative systems, i.e. inelastic hard spheres and inelastic Maxwell particles. There is a strong emphasis on the latter models because that is the area where most of the interesting new developments occurred. In systems of Maxwell particles the collision frequency is independent of the relative velocity of the colliding particles, and in hard sphere systems it is linear. We then demonstrate the existence of scaling solutions for the velocity distribution function, $F(v,t) \sim v_0(t)^{-d} f((v/v_0(t))$, where v_0 is the r.m.s. velocity. The scaling form $f(c)$ shows overpopulation in the high energy tails. In the case of freely cooling systems the tails are of algebraic form, $f(c) \sim c^{-d-a}$, where the exponent a may or may not depend on the degree of inelasticity, and in the case of forced systems the tails are of stretched Gaussian type $f(v) \sim \exp[-\beta(v/v_0)^b]$ with $b < 2$.

1 Introduction

The interest in granular fluids [1] and gases has led to a great revival in kinetic theory of dissipative systems [2, 3, 4, 5], in particular in the non-equilibrium steady states of such systems. A granular fluid [6] is a collection of small or large macroscopic particles with short range hard core repulsions, which lose energy in inelastic collisions, and the system cools without constant energy input.

As energy is not conserved in inelastic collisions Gibbs' equilibrium statistical mechanics is not applicable, and non-equilibrium statistical mechanics and kinetic theory for such systems have to be developed to describe and understand the wealth of interesting phenomena discovered in such systems. The inelasticity is responsible for a lot of new physics, such as clustering and spatial heterogeneities [7], inelastic collapse and the development of singularities within a finite time [8, 9], spontaneous formations of patterns and phase transitions [10], overpopulated non-Gaussian high energy tails in distribution functions [11, 12, 13], break down of molecular chaos [7, 14], single peak initial distributions developing into stable two-peak distributions as the inelasticity decreases, at least in one-dimensional systems [15, 16]. These phenomena have been studied in laboratory experiments [13], by Molecular Dynamics [7, 14, 15] or Monte Carlo simulations [17, 18, 15, 19], and by kinetic theory methods (see recent review [20] and references therein).

The prototypical model for granular fluids or gases is a system of mono-disperse, smooth inelastic hard spheres, which lose a fraction of their relative kinetic energy in every collision, proportional to the degree of inelasticity $(1-\alpha^2)$, where α with $0 \leq \alpha \leq 1$ is the coefficient of restitution. The model is a well-defined microscopic N particle model, which can be studied by molecular dynamics, and by kinetic theory. The single particle distribution function can be described by the nonlinear Boltzmann equation for inelastic hard spheres [2, 3].

The present article presents a review of kinetic theory studies, dealing with the *early* stages of local relaxation of the velocity distribution $F(v,t)$, and we avoid the long time hydrodynamic regime where gradients in density and flow fields are important. So, we restrict our study to *spatially homogeneous states*. Without energy supply these systems are freely cooling [21, 11, 12]. When energy is supplied to the system a source or forcing term is added to the Boltzmann equation [22, 14, 12, 18], and the kinetic equation allows steady state solutions, which depend on the mode of energy supply [22, 14, 12, 18].

A freely evolving inelastic gas or fluid relaxes within a mean free time to a homogeneous cooling state, where it can be described by a scaling or similarity solution of the Boltzmann equation, $F(v,t) \sim (1/v_0(t))^d f(v/v_0(t))$. Such solutions depend on a single scaling variable $c = v/v_0(t)$ where $v_0(t)$ is the r.m.s. velocity or instantaneous width of the distribution. This early evolution is comparable to the rapid decay of the distribution function to a Maxwell-Boltzmann distribution in an spatially homogenous elastic system. However, in systems of elastic particles similarity solutions of the nonlinear homogeneous Boltzmann equation do *not* control the long time behavior of $F(v,t)$ [23]. The earlier studies [21, 11, 12] of these problems were mainly focussing on inelastic hard spheres, which is the proto-typical model for inelastic gases and fluids, and on the extremely simplified inelastic BGK-models with a single relaxation time [24].

More recently simplified stochastic models have been introduced [25, 26, 27] to tackle the nonlinear Boltzmann equation, while keeping the essential physics of the inelastic collisions. Unfortunately the microscopic dynamics of these stochastic models is only defined for velocity variables, and the models can not be studied in phase space using the $N-$particle methods of statistical mechanics and molecular dynamics.

Nevertheless, the recent studies of inelastic Maxwell models [28, 29, 30, 31, 32, 33, 34, 35, 36, 37, 38, 39, 40, 41] have greatly advanced our understanding of kinetic theory for inelastic systems, as well as the structure of the resulting velocity distributions and the significance of scaling solutions, which are exposing the generic features of relaxation both in homogeneous cooling states, as well as in driven systems.

The physical importance of these scaling solutions has been demonstrated by Baldassarri et al. [28, 29, 30] with the help of MC simulations of the nonlinear Boltzmann equation for one- and two-dimensional systems of inelastic Maxwell particles. They found that the solution, $F(v,t)$, after a short transient time, could be collapsed on a scaling form $v_0^{-d}(t)f(v/v_0(t))$ for large classes of initial distributions $F(v,0)$ (e.g. uniform or Gaussian). Moreover, in one dimension they found a simple exact scaling solution of the Boltzmann equation, which has a heavily over-populated algebraic tail $\sim v^{-4}$ when compared to a Gaussian. In two dimensions they have shown that the solutions of the initial value problem for regular initial distributions (say, without tails) also approach a scaling form with over-populations in the form of algebraic tails, $f(c) \sim c^{-d-a}$ with an exponent $a(\alpha)$ that depends on the degree of inelasticity α.

In the same period Krapivsky and Ben-Naim [31, 32, 33], and independently the present authors [34, 35, 37] developed analytic methods to determine the scaling solutions of the nonlinear Boltzmann equation for freely evolving Maxwell models, and in particular to calculate the exponent $a(\alpha)$ of the high energy tails $f(c) \sim 1/c^{a+d}$, as a function of the coefficient of restitution α. Using the methods of Ref. [12] the present authors have also extended the above results to inelastic Maxwell models driven by different modes of energy supply [36]. Here the high energy tails turned out to be stretched Gaussians, $f(c) \sim \exp[-\beta c^b]$ with $0 < b < 2$. Very recently these studies were also generalized to inelastic soft spheres [37, 19] both for freely evolving as well as for driven systems, where the over-populated high energy tails turn out to be stretched Gaussians with $0 < b < 2$ as well. This class of models covers both inelastic hard spheres and inelastic Maxwell models as special cases. We will only briefly touch upon these models in the concluding section of this article.

Subsequently there appeared also rigorous mathematical proofs of the approach to these scaling forms for freely evolving inelastic Maxwell gases [39], for inelastic hard sphere gases driven by white noise [40], and for both types of systems driven by different types of thermostats [41].

This discovery stimulated a lot of theoretical and numerical research in solutions of the Boltzmann equation, specially for large times and for large velocities, as universal phenomena manifest themselves mostly on such scales. Why were the first results all for Maxwell models? Maxwell models [23] derive their importance in kinetic theory from the property that the collision frequency is independent of the relative impact speed g, whereas the collision frequency in general depends on the speed at impact. For instance, for hard spheres the collision frequency is proportional to g.

This property of Maxwell models simplifies the structure of the nonlinear kinetic equation. For instance, the equations of motion for the moments $\langle v^n \rangle$ can be solved sequentially as an initial value problem; the eigenvalues and eigenfunctions of the linearized collision operator can be calculated, and the $(2d-1)-$dimensional nonlinear collision integral in the Boltzmann equation can be reduced to a $(d-1)-$dimensional one by means of Fourier transformation [26]. In subsequent sections we will take advantage of these properties to determine similarity solutions of the nonlinear Boltzmann equation for the $d-$dimensional IMM, and the moment equations enable us to study the approach of initial value solutions $F(v,t)$ to such similarity solutions.

The plan of the paper is as follows: In Sections 2 and 3 the nonlinear Boltzmann equation for a one-dimensional gas of Maxwell particles is solved without and with energy input to obtain scaling solutions. The high energy tails are respectively power laws or stretched Gaussian tails. Section 4 is an intermezzo about an inelastic BGK-kinetic equation without or with energy supply, for which the high energy tails are analyzed. After discussing in Section 5 the basics of the nonlinear Boltzmann equation for our two fundamental $d-$dimensional inelastic models, i.e. inelastic Maxwell models (IMM) and inelastic hard spheres (IHS), we repeat the above program for $d-$dimensional models in Section 6 for free cooling, and in Section 8 for driven Maxwell models. In the intermediate Section 7 we study the approach of the velocity distribution function $F(v,t)$ towards the scaling solution, and Section 9 gives some conclusions and perspectives.

2 Freely cooling one-dimensional gases

2.1 Nonlinear Boltzmann equation

Some of the basic features of inelastic systems can be discussed using the Boltzmann equation for a simple one-dimensional model [25] with inelastic interactions, possibly driven by Gaussian white noise. Let us denote the isotropic velocity distribution function at time t by $F(v,t) = F(|v|,t)$. Its time evolution is described by the nonlinear Boltzmann equation,

$$\frac{\partial}{\partial t}F(v,t) - D\frac{\partial^2}{\partial v^2}F(v,t) = I(v|F), \tag{2.1}$$

where the diffusion term, proportional to $\partial^2/\partial v^2$, represents the heating effect of Gaussian white noise with strength D. The collision operator, $I(v|F)$, consists of two terms: the loss term, that accounts for the so-called *direct* collisions of a particle with velocity v with any other particle, and the gain term that accounts for the so-called *restituting* collision of two particles with pre-collision velocities v^{**} and w^{**}, resulting in the post-collision velocities (v,w):

$$\begin{aligned} I(v|F) &= \int dw \left[\frac{1}{\alpha}F(v^{**},t)F(w^{**},t) - F(w,t)F(v,t)\right] \\ &= -F(v,t) + \frac{1}{p}\int duF(u,t)F\left(\frac{v-qu}{p},t\right), \end{aligned} \tag{2.2}$$

where $p = 1-q = (1+\alpha)/2$ and α is the coefficient of restitution with $0 \leq \alpha \leq 1$. All velocity integrations in (2.2) extend over the interval $(-\infty,+\infty)$. Because F is normalized to unity, the loss term is simply equal to $-F(v,t)$. Equation (2.2) is the nonlinear Boltzmann for the *Inelastic Maxwell Model* (IMM) in one dimension, introduced by Ben-Naim and Krapivsky [25].

In a *direct collision* two particles with velocities v and w collide, resulting in post-collision velocities, v^* and w^*, given by:

$$\begin{aligned} v^* = v(\alpha) &\equiv \tfrac{1}{2}(1-\alpha)v + \tfrac{1}{2}(1+\alpha)w \qquad \text{or} \qquad v^* = qv + pw \\ w^* = w(\alpha) &\equiv \tfrac{1}{2}(1+\alpha)v + \tfrac{1}{2}(1-\alpha)w \qquad \text{or} \qquad w^* = pv + qw, \end{aligned} \tag{2.3}$$

where total momentum is conserved. The *restituting collisions* are events in which two particles with pre-collisional velocities v^{**} and w^{**} collide such that one of the post-collisional velocities is equal to v. The velocities are given by the inverse transformation of (2.3), i.e. $v^{**} = v(1/\alpha)$ and $w^{**} = w(1/\alpha)$.

The velocity distribution function is normalized such that mass and mean energy or granular temperature are,

$$\int d\boldsymbol{v}\, F(v,t) = 1; \qquad \langle v^2\rangle(t) = \int d\boldsymbol{v}\, v^2 F(v,t) \equiv \tfrac{1}{2}dv_0^2(t). \tag{2.4}$$

For later reference the normalization of the mean kinetic energy is written down for $d-$dimensional systems, where $v_0(t)$ is referred as the r.m.s. velocity, and $T = v_0^2$

as the granular temperature. The evolution equation of the energy $\langle v^2 \rangle$ is obtained by multiplying (2.1) with $\int d\boldsymbol{v} v^2$, which yields,

$$\frac{d}{dt} v_0^2 = 4D - 2pq v_0^2. \tag{2.5}$$

It describes the approach of $v_0^2(t)$ to a non-equilibrium steady state (NESS) with r.m.s. velocity $v_0(\infty) = \sqrt{2D/pq}$. Here the heating rate D due to the random forces is balanced by the loss rate, $\propto pqv_0^2$, caused by the inelastic collisions. The energy balance equation (2.5) has an stable attractive fixed point solution $v_0(\infty)$ in the sense that any $v_0(t)$, with an initial value different from $v_0(\infty)$, approaches this fixed point at an exponential rate. This one-dimensional model Boltzmann equation (2.1) will be extended to general dimensionality d in later sections.

An inelastic fluid without energy input, in the so-called *homogeneous cooling state*, will cool down due to the collisional dissipation. In experimental studies of granular fluids energy has to be supplied at a constant rate to keep the system in a non-equilibrium steady state, while in analytic, numerical and simulation work freely cooling systems can be studied directly. Without energy input the velocity distribution $F(v,t)$ will approach a Dirac delta function $\delta(\boldsymbol{v})$ as $t \to \infty$, and all moments approach zero, including the width $v_0(t)$. However, an interesting structure is revealed when velocities, $c = v/v_0(t)$, are measured in units of the instantaneous width $v_0(t)$, and the long time limit is taken while keeping c constant, the so-called *scaling limit*. *Scaling* or similarity solutions of the Boltzmann equation are special solutions of a single scaling argument $c = v/v_0(t)$, where the normalization of mass requires,

$$F(v,t) = (v_0(t))^{-d} f(v/v_0(t)). \tag{2.6}$$

Consequently $f(c)$ satisfies the normalizations,

$$\int d\boldsymbol{c} f(c) = 1; \qquad \int d\boldsymbol{c}\, c^2 f(c) = \tfrac{1}{2}d. \tag{2.7}$$

To understand the physical processes involved we first discuss in a qualitative way the relevant limiting cases. Without the heating term ($D = 0$), equation (2.1) reduces to the freely cooling IMM. If one takes in addition the elastic limit $q \to 0$, the collision laws reduce in the *one-dimensional* case to $v^* = w, w^* = v$, i.e. an exchange of particle labels, the collision term vanishes identically, so that every $F(v,t) = F(v)$ is a solution, and there is no randomization or relaxation of the velocity distribution through collisions, and the model becomes trivial at the Boltzmann level of description. However, the distribution function in the presence of *infinitesimal* dissipation ($\alpha \to 1$) approaches a Maxwellian. If we turn on the noise ($D \neq 0$) at vanishing dissipation ($q = 0$), the r.m.s. velocity in (2.5), $v_0^2(t) = v_0^2(0) + 4Dt$, is increasing linearly with time. With stochastic heating *and* dissipation (even in infinitesimal amounts) the system reaches a NESS, through the balance of energy input and dissipation.

2.2 Scaling solutions

After this qualitative introduction into the physical processes, we will study scaling solutions (2.6) of the nonlinear Boltzmann equation in a freely evolving system without energy input ($D = 0$). We first take the Fourier transform of the Boltzmann equation (2.1). Because of the convolution structure of the nonlinear collision term (2.2) it reduces to

$$\frac{\partial}{\partial t}\Phi(k,t) = -\Phi(k,t) + \Phi(kq,t)\Phi(kp,t). \tag{2.8}$$

This equation possesses an interesting scaling or similarity solution of the form, $\Phi(k,t) = \phi(kv_0(t))$, which is the equivalent of (2.6) in Fourier representation. Substitution of this ansatz into (2.8) yields then,

$$-pqk\phi'(k) = -\phi(k) + \phi(qk)\phi(pk), \tag{2.9}$$

where the energy balance equation (2.5) has been used to eliminate dv_0/dt. By combining solutions of the form $(1 - sk)e^{sk}$ for positive and negative k, one can construct a special solution of (2.9) as: $\phi(k) = (1 + s|k|)\exp[-s|k|]$, with an inverse Fourier transform [28] given by

$$f(c) = \frac{2}{\pi s}\frac{1}{[1 + c^2/s^2]^2}. \tag{2.10}$$

By choosing $s = 1/\sqrt{2}$, one obtains the scaling solution that obeys the normalization $\langle c^2 \rangle = \frac{1}{2}$, as imposed by (2.4). The solution above has an algebraic form; it is even in the velocity variable, with a power law tail $1/c^4$ at high energy, and moments of order larger than 2 are all *divergent*. Notice that the solution (2.10) does not depend on the inelasticity, which is an exceptional property of the freely evolving inelastic Maxwell model in one dimension, as we shall see in later sections.

2.3 Moment equations and approach to scaling

An enormous simplification of both elastic and inelastic Maxwell models, as compared to hard spheres or other interaction models, is that the infinite set of moment equations can be solved sequentially as an initial value problem. This enables us to investigate analytically, at least to some extent, how the general solution $F(v,t)$ of the complex nonlinear Boltzmann equation approaches the much simpler scaling solution $f(c)$ of a single scaling variable.

From general considerations we know already that the solution $F(v,t)$ of the inelastic Boltzmann equation approaches a delta function. So, all its moments must vanish in the long time limit, whereas the moments $\langle c^n \rangle$ of the scaling form are constant for $n = 0, 2$, and divergent for $n > 2$ on account of (2.10).

In our subsequent analysis it is convenient to define the standard moments $m_n(t)$ and the rescaled moments $\mu_n(t)$ of the distribution function as,

$$m_n(t) \equiv v_0^n \mu_n(t) = \frac{1}{n!} \int dv\, v^n F(v,t). \tag{2.11}$$

The evolution equation of the moments can be obtained by multiplying (2.1) by v^n and integrating over v, i.e.:

$$\frac{dm_n}{dt} = -m_n + \frac{1}{p\, n!} \int \int dv du\, v^n F(u,t) F\left(\frac{v - qu}{p}, t\right). \tag{2.12}$$

After a simple change of variables, the gain term in this equation transforms into,

$$\frac{1}{n!} \int \int du dw (pw + qu)^n F(u,t) F(w,t) = \sum_{l=0}^{n} p^l q^{n-l} m_l m_{n-l}, \tag{2.13}$$

where we have used Newton's binomial formula. We first observe that particle conservation gives $m_0(t) = 1$. Combination of (2.12) and (2.13) yields the moment equations,

$$\frac{dm_n}{dt} + \lambda_n m_n = \sum_{l=2}^{n-2} p^l q^{n-l} m_l m_{n-l}, \tag{2.14}$$

where the eigenvalue λ_n is given by,

$$\lambda_n = 1 - p^n - q^n. \tag{2.15}$$

Next we observe that for an isotropic $F(|v|,t)$ only the even moments are nonvanishing. So, (2.14) only involves even values of l and n. This set of equations can be solved recursively for all n. For $n = 2$ the nonlinear term on the right hand side vanishes, and we find,

$$m_2(t) = m_2(0) e^{-\lambda_2 t} \tag{2.16}$$

with $\lambda_2 = 2pq$. We note that $m_2(t) = v_0^2(t)/4$. Similarly we solve the equation for the fourth moment,

$$m_4(t) = \left[m_4(0) + \tfrac{1}{2} m_2^2(0)\right] \exp[-\lambda_4 t] - \tfrac{1}{2} m_2^2(0) \exp[-\lambda_2 t], \tag{2.17}$$

where the equality $\lambda_4 - 2\lambda_2 = -2p^2q^2$ has been used. The coefficients in (2.17) turn out to be independent of p and q. Similarly we can show that the dominant long time behavior of the higher even moments is given by $m_n(t) \sim \exp[-\lambda_n t]$, i.e. they decay asymptotically according to (2.14) with the nonlinear right hand side set equal to zero. This is the multi-scaling behavior of the velocity moments found by Ben-Naim and Krapivsky in [25, 33]. Consequently all moments with $n > 0$ vanish as $t \to \infty$, consistent with the fact that the distribution $F(v,t) \to \delta(v)$ in this limit.

The approach of $F(v,t)$ to a scaling form in $d-$dimensional inelastic models was first formulated and conjectured by the present authors based on their analysis of the time evolution of the moments (for inelastic hard spheres and inelastic Maxwell models see [35]; extended to inelastic soft spheres [37, 19]), and was subsequently proven in a mathematically rigorous fashion for inelastic Maxwell models and hard spheres [39, 40, 41]. Rather than presenting the mathematical proof it is of more interest from the physics point of view to understand how the physically most important lower moments of $F(v,t)$ approach their limiting form, and relate these limits to the moments of the scaling solution (2.10).

We first observe that the assumed large$-t$ behavior (2.6) of $F(v,t)$ in combination with (2.11) implies that $\mu_n(t) \to \mu_n$ for $n = 2, 4 \ldots$, where $\mu_n \equiv (1/n!) \int dc\, c^n f(c)$. So, the moment equations for the rescaled moments follow directly from (2.14) and (2.11) to be,

$$\frac{d\mu_n(t)}{dt} + \gamma_n \mu_n(t) = \sum_{l=2}^{n-2} p^l q^{n-l} \mu_l(t) \mu_{n-l}(t), \tag{2.18}$$

with eigenvalue

$$\gamma_n = \lambda_n - \tfrac{1}{2} n \lambda_2 \tag{2.19}$$

on account of (2.14) and (2.16). For $n = 2$ one obtains that $\mu_2(t) = \mu_2 = \frac{1}{2}\langle c^2 \rangle = \frac{1}{4}$ is constant for all times, in agreement with the corresponding moment of the scaling form (2.10). Next we consider the fourth moment $\mu_4(t)$, which follows immediately from (2.17) and (2.11) and reads,

$$\mu_4(t) = m_4(t)/v_0^4(t) = -\tfrac{1}{2}\mu_2^2 + \exp(2p^2q^2t)[\mu_4(0) + \tfrac{1}{2}\mu_2^2]. \tag{2.20}$$

This solution is indeed *positive* and finite for all finite positive times, and approaches $+\infty$ as t becomes large. A similar result for the time dependence of $\mu_n(t)$ is obtained from (2.18) for $n = 6, 8, \cdots$. This behavior is fully consistent with the exact scaling solution (2.10), of which all even moments with $n > 2$ are divergent.

Now, a curious result follows by considering the stationary solutions of (2.18) by setting $d\mu_n(t)/dt = 0$. The equations then reduce to a simple recursion relation,

$$\mu_n = \frac{1}{\gamma_n} \sum_{l=2}^{n-2} p^l q^{n-l} \mu_l \mu_{n-l} \tag{2.21}$$

with initialization, $\mu_2 = \frac{1}{4}$. This yields for $n = 4$,

$$\mu_4 = \frac{p^2 q^2}{\gamma_4} \mu_2^2 = -\frac{1}{32}, \tag{2.22}$$

where we have used the relation $\gamma_4 = -2p^2q^2$, as follows from (2.15). A *negative* moment of a physical (positive) distribution is clearly *unphysical*. This unphysical behavior continues for higher moments, where one finds in a similar manner that the even moments approach a *finite* value, $\mu_{2n} \propto (-)^{n+1}\mathcal{C}_n$, with alternating signs!

What is happening here? Clearly, the set of solutions $\{\mu_{2n}\}$ of the limiting equation (2.21) *differs* from the long time limit $\mu_{2n}(\infty)$ of the set of solutions $\mu_{2n}(t)$ of (2.18). The fixed point solution $\{\mu_n, n = 2, 4, \ldots\}$ of (2.21) does not represent a *stable attracting* fixed point for physical solutions, but an unstable/repelling one. The physical solutions $\mu_n(t)$ of (2.18) move for large t away from the unstable fixed point $\{\mu_n\}$ at an exponential rate, given by $\exp(2p^2q^2t)$.

3 Driven 1-D gases

In this section we discuss the scaling form of the velocity distribution in the non-equilibrium steady state (NESS) for the one-dimensional IMM for different modes of energy supply, and the results are compared with those of the proto-typical dissipative fluid of hard spheres in one dimension. In general, a NESS can be reached when the energy loss through collisional dissipation is compensated by energy supplied externally, as described in (2.5) for the case of external Gaussian white noise. This stationary case is described by the Boltzmann equation (2.1) with $\partial_t F(v,t) = 0$. Moreover, at the end of this section all known results for scaling forms in *driven* inelastic one-dimensional systems will be summarized.

To obtain a description of the NESS, that is independent of the details of the initial state, we rescale velocities, $c = v/v_0(\infty)$, in terms of the r.m.s. velocity $v_0(\infty)$, and express $F(v,\infty)$ in terms of the scaling form $f(c)$ introduced in (2.6). The Boltzmann equation (2.1) then takes the form,

$$-\frac{D}{v_0^2(\infty)} \frac{d^2 f}{dc^2} = -\tfrac{1}{2} pq \, d^2 f(c)/dc^2 = I(c|f), \tag{3.1}$$

where $v_0(\infty) = \sqrt{2D/pq}$. The integral equation for the characteristic function, $\phi(k) = \int dc\, e^{-ikc} f(c)$, follows by taking the Fourier transform of the above equation,

$$(1 + \tfrac{1}{2}\, pqk^2)\phi(k) = \phi(pk)\phi(qk), \tag{3.2}$$

where the nonlinear collision term has been obtained as in (2.8). An exact scaling solution of this equation in the form of an infinite product has been obtained by Ben-Naim and Krapivsky [25, 33], and by Nienhuis and van der Hart [42]. Here we construct the solution following Santos and Ernst in [43]. We multiply (3.2) on both sides with $\phi_0(k) \equiv 1/(1 + \frac{1}{2}pqk^2)$, and write the equation as an iteration scheme,

$$\phi_{n+1} = \phi_0(k)\phi_n(pk)\phi_n(qk). \tag{3.3}$$

The solution can be found iteratively by starting from $\phi_0(k)$, and inserting $\phi_n(k)$ on the right hand side to obtain $\phi_{n+1}(k)$ on the left hand side. The result is the infinite product,

$$\phi(k) = \prod_{m=0}^{\infty} \prod_{\ell=0}^{m} \left(1 + k^2/k_{m\ell}^2\right)^{-\nu_{ml}}, \tag{3.4}$$

where $\nu_{m\ell} \equiv \begin{pmatrix} m \\ \ell \end{pmatrix}$ and $k_{m\ell} \equiv ap^{-\ell} q^{-(m-\ell)}$ with $a \equiv \sqrt{2/pq}$. Thus $\phi(k)$ has infinitely many poles at $k = \pm i k_{m\ell}$ on the imaginary axis with multiplicity $\nu_{m\ell}$ (for $\alpha \neq 0$). The velocity distribution,

$$f(c) = \frac{1}{2\pi} \int_{-\infty}^{\infty} dk\, e^{ikc} \phi(k), \tag{3.5}$$

can then be obtained by contour integration. As $f(c)$ is an even function, we only need to evaluate the integral in (3.5) for $c > 0$. The replacement $c \to |c|$ gives then the result for all c. By closing the contour by a semi-circle through the infinite upper half-plane and applying the residue theorem we obtain the exact solution in the form of an infinite sum over poles. This representation of $f(c)$ is very well suited to discuss the high energy tail.

The dominant terms for large $|c|$ correspond the poles closest to the real axis, i.e. to the smallest values of $k_{m\ell}$. In case $\alpha \neq 0$ the two smallest values are $k_{00} = a$ and $k_{11} = a/p$. Consequently, the leading and first subleading term are

$$f(c) \approx A_0 e^{-a|c|} + A_1 e^{-(a/p)|c|} + \cdots, \tag{3.6}$$

where $a = \sqrt{2/pq}$ and the coefficients are found as

$$A_0 = \frac{a}{2} \prod_{n=0}^{\infty} \exp\left[\left(\frac{1}{n+1} \right) \frac{p^{2(n+1)} + q^{2(n+1)}}{1 - p^{2(n+1)} - q^{2(n+1)}} \right]$$

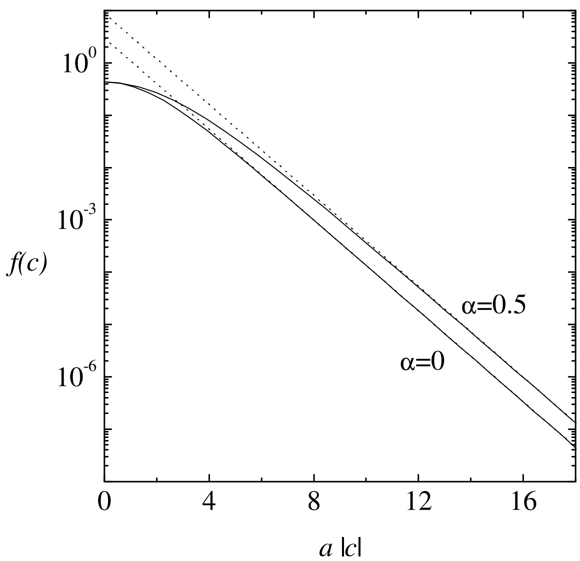

Figure 1: Logarithmic plot of $f(c)$ versus $a|c|$ for $\alpha = 0$ and $\alpha = 0.5$. The dotted lines are the asymptotic forms $f(c) \approx A_0 e^{-a|c|}$ at $\alpha = 0$ and $\alpha = 0.5$, obtained from (3.7).

$$
\begin{aligned}
A_1 &= (-)\frac{ap^3}{2(1-p^2)(p-q)} \\
&\quad \times \prod_{n=0}^{\infty} \exp\left[\left(\frac{p^{-2(n+1)}}{n+1}\right)\frac{\left(p^{2(n+1)}+q^{2(n+1)}\right)^2}{1-p^{2(n+1)}-q^{2(n+1)}}\right].
\end{aligned} \tag{3.7}
$$

In conclusion, the scaling form $f(c)$ in driven one-dimensional IMM systems shows again an *overpopulated* high energy tail $\sim \exp(-a|c|)$, when compared to a Gaussian. However this overpopulation is very much smaller than in the freely cooling case, where $f(c) \sim 1/c^4$ for large c.

Figure 1 compares the asymptotic form $f(c) \approx A_0 e^{-a|c|}$ with the function $f(c)$ obtained by numerically inverting $\phi(k)$ in (3.2) for $\alpha = 0$ and $\alpha = 0.5$. Similar results have been obtained by Nienhuis and van der Hart [42] and by Antal et al. [44]. We observe that the asymptotic behavior is reached for $a|c| \gtrsim 4$ if $\alpha = 0$ and for $a|c| \gtrsim 8$ if $\alpha = 0.5$. As $a = \sqrt{2/pq}$ this corresponds to velocities far above the r.m.s. velocity.

Interesting limiting behavior is also found in the *quasi-elastic* limit. This limit is much more delicate and requires some care. If we first take $\alpha \to 1$ at fixed $|c|$ and next $|c| \to \infty$ (denoted as order A in Table I), the high energy tail has a Maxwellian form. On the other hand, if the limits are taken in the reverse order,

State	System	Order A	Order B
Free cooling	Hard spheres[1, 2]	$\frac{1}{2}\left[\delta(c+c_0)+\delta(c-c_0)\right]$	$e^{-a\lvert c\rvert}$
	Maxwell model[3, 3]	c^{-4}	c^{-4}
White noise	Hard spheres[1, 4]	$e^{-a\lvert c\rvert^3}$	$e^{-a\lvert c\rvert^{3/2}}$
	Maxwell model[5, 6]	e^{-ac^2}	$e^{-a\lvert c\rvert}$
Gravity thermostat	Hard spheres[5, 7]	$\frac{1}{2}\left[\delta(c+c_0)+\delta(c-c_0)\right]$	e^{-ac^2}
	Maxwell model[5, 8]	$\frac{1}{2}\left[\delta(c+c_0)+\delta(c-c_0)\right]$	$e^{-a\lvert c\rvert}$

Table 1: Asymptotic behavior of the 1-D scaling form $f(c)$ in the quasi-elastic limit for orders A and B. The first/second footnote in the second column gives the reference where the result for order A/B was obtained. References: [1] Ref. [15], [2] Ref. [12], [3] Refs. [28, 25, 34], [4] Refs. [12, 15], [5] Ref.[43], [6] Refs. [15, 36], [7] Ref.[18], [8] Ref. [36].

i.e. first $|c| \to \infty$ at fixed $\alpha < 1$ and then $\alpha \to 1$ (denoted as order B in Table I), the asymptotic high energy tail is exponential. The crossover between both limiting behaviors is roughly described by the coupled limit $c \to \infty$ and $q \to 0$ with the scaling variable $w = |c|\sqrt{q} =$ fixed with $q \equiv \frac{1}{2}(1-\alpha) \ll 1$, and occurs at $w \simeq 1$. If $w < 1$ the distribution function is essentially a Maxwellian, while the true exponential high energy tail is reached if $w \gg 1$.

The results for the scaling form in the quasi-elastic limit not only depend sensitively on the order in which both limits are taken. They also depend strongly on the collisional interaction, i.e. on the energy dependence of the collision frequency, as well as on the mode of energy supply to the system.

To illustrate this we have collected in Table I what is known in the literature for the different inelastic models in one dimension: (i) hard spheres and (ii) Maxwell models, and for different modes of energy supply: (i) no energy input or free cooling, (ii) energy input or driving through Gaussian white noise, represented by the forcing term $-D\partial^2 F(v,t)/\partial v^2$ in Boltzmann equation (2.1), and (iii) energy input through a *negative* friction force $\propto \zeta v/|v|$, acting in the direction of the particle's velocity, but independent of its speed. This forcing term, referred to as gravity thermostat in [18], can be represented by a forcing term, $\zeta(d/dv)(v/|v|)F(v,t)$, in the Boltzmann equation. The results for the gravity thermostat corresponding to order A have been obtained by the same method as followed in Ref. [15].

Inelastic gases in one dimension exhibit the remarkable property that single peaked initial distributions develop into double peaked solutions as the inelasticity decreases [15, 16]. It is worthwhile to note that in the quasi-elastic limit a bimodal distribution, $\frac{1}{2}\left[\delta(c+c_0)+\delta(c-c_0)\right]$ with $c_0 = 1/\sqrt{2}$, is observed in inelastic hard sphere systems both for free cooling and for driving through the gravity thermostat. In inelastic Maxwell models however, this bimodal distribution is only observed for the gravity thermostat.

It is also important to note that in the normalization where velocities are measured in units of the r.m.s. velocity, the high energy tail in the driven inelastic Maxwell model is only observable for very large velocities, as illustrated in Figure 1 for strong ($\alpha \to 0$) and intermediate ($\alpha = \frac{1}{2}$) inelasticity. In the quasi-elastic limit, where ($\alpha \to 1$), the tail is even pushed further out towards infinity. This also explains how to reconcile the paradoxical results of *exponential* large-c behavior with the very accurate representation of the distribution function in the thermal range ($c \simeq 1$), in the form of a Maxwellian, multiplied by a polynomial expansion in Hermite or Sonine polynomials with coefficients related to the cumulants (see Refs. [43]). The validity of these polynomial expansions, over a large range of inelasticities with ($0 \leq \alpha < 1$) has been observed before in [12] for inelastic hard spheres and in [27] for inelastic Maxwell models. Derivations of the results, collected in Table I can be found in the original literature.

4 Inelastic BGK-Model

A brief intermezzo on a very simple inelastic Bhatnagar-Gross-Krook (BGK) model, introduced by Brey et al. [24], is presented here to show to what extent this model captures the correct physics as described by the nonlinear Boltzmann equation for $d-$dimensional inelastic Maxwell models.

A crude scenario for relaxation without energy input has to show that the system cools down due to inelastic collisions, and that the velocity distribution $F\left(v,t\right)$ approaches a Dirac delta function $\delta\left(\boldsymbol{v}\right)$ as $t \to \infty$, while the width or r.m.s. velocity $v_0\left(t\right)$ of this distribution, defined as $\langle v^2 \rangle = \frac{1}{2} d v_0^2$, is shrinking. Moreover with a constant supply of energy, the system should reach a non-equilibrium steady state (NESS). These features are implemented in a simple BGK-equation, i.e.

$$\partial_t F\left(v,t\right) - D\nabla^2_{\boldsymbol{v}} F\left(v,t\right) = -\omega_0 \left[F\left(v,t\right) - F_0\left(v,t\right)\right]. \tag{4.1}$$

Here ω_0 is the mean collision frequency, which is chosen here as $\omega_0 = 1$ in order to model Maxwell models. The terms $-\omega_0 F(v,t)$ and $\omega_0 F_0(v,t)$ model respectively the loss and (nonlinear) gain term. This kinetic equation describes the relaxation of $F\left(v,t\right)$ towards a Maxwellian with a width proportional to $\alpha v_0\left(t\right)$, defined by

$$F_0\left(v,t\right) = \left(\sqrt{\pi}\alpha v_0\right)^{-d} \exp\left[-\left(v/\alpha v_0\right)^2\right] \equiv \left(\alpha v_0\right)^{-d} \phi\left(c/\alpha\right), \tag{4.2}$$

where $c = v/v_0$. The energy balance equation follows from (4.1) as,

$$dv_0^2/dt = 4D - (1-\alpha^2)v_0^2 \equiv 4D - 2\gamma v_0^2, \tag{4.3}$$

where $(1 - \alpha^2)$ measures the inelasticity. In the case of *free cooling* ($D = 0$) the solution is $v_0(t) = v_0(0) \exp[-\gamma t]$. By inserting the scaling ansatz (2.6) into (4.1) we obtain in the case of free cooling an ordinary differential equation, that can be solved exactly [24, 37, 19]. Its high energy tail is,

$$f(c) \sim A/c^{a+d} \quad \text{with} \quad a = 1/\gamma = 2/(1-\alpha^2), \tag{4.4}$$

where an explicit expression for the amplitude A has been calculated.

As we shall see in Section 6, a similar heavily overpopulated tail, $f(c) \sim 1/c^{d+a}$ for $d > 1$, has also be found in freely cooling $d-$dimensional Maxwell models with $\omega_0 = 1$, where the exponent $a(\alpha)$ takes for small inelasticity the form $a \simeq 1/\gamma_0 = 4d/\left(1-\alpha^2\right)$.

For the BGK-model *driven* by external white noise we obtain a NESS with a rescaled distribution function $F(v, \infty) = v_0^{-d}(\infty) f(v/v_0(\infty))$ with standard width $\langle c^2 \rangle = \frac{1}{2}d$, and the rescaled equation for $f(c)$ is obtained from (4.1). Its asymptotic solution for $c \gg \alpha$ is then,

$$f(c) \sim \exp\left[-\beta c^b\right] = \exp\left[-2c/\sqrt{1-\alpha^2}\right]. \tag{4.5}$$

As we shall see in Section 8, a similar exponential high energy tail is found in the white noise driven Maxwell models .

5 d-Dimensional inelastic Maxwell gases

In this section we consider the spatially homogeneous Boltzmann equation for inelastic Maxwell models in d dimensions without energy input. In most models of inelastic particles total momentum is conserved in binary collisions, and the models qualify as inelastic fluids. The details of the collision dynamics are defined in Figure 2. The nonlinear Boltzmann equation for a d-dimensional IMM when driven by Gaussian white noise can again be written in the form,

$$\frac{\partial}{\partial t}F(v,t) - D\nabla_{\boldsymbol{v}}^2 F(v,t) = I(v|F), \tag{5.1}$$

where the collision term is,

$$I(v|F) = \int_n \int d\boldsymbol{w} \left[\frac{1}{\alpha}F(v^{**},t)F(w^{**},t) - F(v,t)F(w,t)\right] \tag{5.2}$$

Here $\int_n(\cdots) = (1/\Omega_d)\int d\boldsymbol{n}(\cdots)$ is an angular average over a full d-dimensional unit sphere with a surface area $\Omega_d = 2\pi^{d/2}/\Gamma(d/2)$. The factor $(1/\alpha)$ in the gain

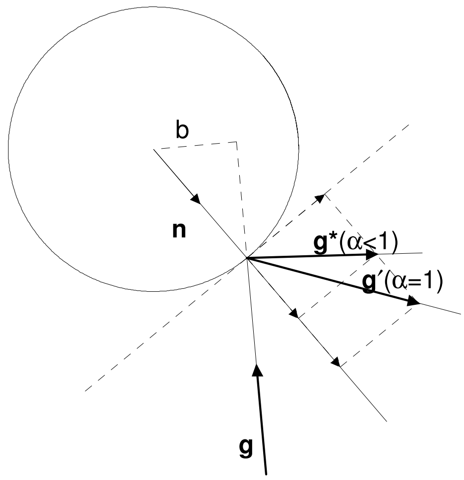

Figure 2: Geometry of inelastic collisions, where $\boldsymbol{g} = \boldsymbol{v} - \boldsymbol{w}$ is the relative velocity, the unit vector $\boldsymbol{n}$ specifies the point of incidence on a unit sphere around the centre of force, $b = |\hat{\boldsymbol{g}} \times \boldsymbol{n}| = |\sin\theta|$ is the impact parameter, and θ the angle of incidence. In inelastic collisions the component $g_{\|} = \boldsymbol{g} \cdot \boldsymbol{n} = g\cos\theta$ is reflected, i.e. $g_{\|}^{*} = -\alpha g_{\|}$, and reduced in size by a factor $\alpha = 1 - 2q = 2p - 1$, where α is called the coefficient of restitution ($0 \leq \alpha \leq 1$), and $\alpha = 1$ corresponds to the elastic case. If the total energy in a collision is $E = \frac{1}{2}(v^2 + w^2)$, then the energy loss in an inelastic collision is $\Delta E = -\frac{1}{4}(1-\alpha^2)g_{\|}^2 = -pqg_{\|}^2$.

term of (5.2) originates from the Jacobian, $d\boldsymbol{v}^{**}d\boldsymbol{w}^{**} = (1/\alpha)d\boldsymbol{v}d\boldsymbol{w}$. The direct and restituting collisions are given by:

$$\begin{aligned} \boldsymbol{v}^* &= \boldsymbol{v} - \tfrac{1}{2}(1+\alpha)(\boldsymbol{g}\cdot\boldsymbol{n})\boldsymbol{n}; \qquad & \boldsymbol{w}^* &= \boldsymbol{w} + \tfrac{1}{2}(1+\alpha)(\boldsymbol{g}\cdot\boldsymbol{n})\boldsymbol{n}, \\ \boldsymbol{v}^{**} &= \boldsymbol{v} - \tfrac{1}{2}(1+\tfrac{1}{\alpha})(\boldsymbol{g}\cdot\boldsymbol{n})\boldsymbol{n}; \qquad & \boldsymbol{w}^{**} &= \boldsymbol{w} + \tfrac{1}{2}(1+\tfrac{1}{\alpha})(\boldsymbol{g}\cdot\boldsymbol{n})\boldsymbol{n}. \end{aligned} \tag{5.3}$$

In one dimension the dyadic product $\boldsymbol{nn}$ can be replaced by unity, so that the equations above reduce to (2.3).

To point out the differences between the Boltzmann equation for inelastic Maxwell particles and the one for the prototypical inelastic hard spheres we also quote the Boltzmann collision term for inelastic hard spheres, i.e.

$$I(v|F) = \int_n \int d\boldsymbol{w}|\boldsymbol{g}\cdot\boldsymbol{n}| \left[\frac{1}{\alpha^2}F(v^{**},t)F(w^{**},t) - F(v,t)F(w,t)\right]. \tag{5.4}$$

Here the collision term contains an extra factor $|\boldsymbol{g}\cdot\boldsymbol{n}|$, and the gain term an extra factor $1/\alpha$ as compared to (5.2). The velocity distributions in these inelastic models with or without energy input were recently studied by many authors; in particular the inelastic hard sphere gas in [22, 11, 12, 17, 18, 15, 36] and the inelastic Maxwell models in [25, 26, 27, 28, 31, 34, 35, 42, 44, 43].

We return to the IMM and observe that in any inelastic collision an amount of energy $\frac{1}{4}(1-\alpha^2)g_{\parallel}^2 = pqg_{\parallel}^2$ is lost. Consequently the average kinetic energy or granular temperature v_0^2 keeps decreasing at a rate proportional to the inelasticity $\frac{1}{4}(1-\alpha^2) = pq$. The balance equation can be derived in a similar manner as (2.5), and reads for general dimensionality,

$$\frac{d}{dt}v_0^2 = 4D - (2pq/d)v_0^2. \tag{5.5}$$

We will discuss *freely cooling* systems $(D = 0)$ without energy input, as well as *driven* systems (see Section 7), which can reach a non-equilibrium steady state. In the case of free cooling the solution of the Boltzmann equation does not reach thermal equilibrium, described by a Maxwellian, but is approaching a Dirac delta function $\delta^{(d)}(\boldsymbol{v})$ for large times. However, the arguments given in Section 2 suggest again that $F(v,t)$ approaches a simple scaling solution of the form $f(c)$, as defined in (2.6) after rescaling the velocities as $c = v/v_0(\infty)$, with normalizations chosen as in (2.7).

In the case of free cooling the mean square velocity keeps decreasing at an exponential rate, $v_0(t) = v_0(0)\exp[-pqt/d]$, but the distribution function rapidly reaches a (time independent) scaling form $f(c)$, which is determined by the non-linear integral equation,

$$\frac{pq}{d}\left(d + c\frac{d}{dc}\right)f = \frac{pq}{d}\boldsymbol{\nabla}_c \cdot (\boldsymbol{c}f) = I(c|f), \tag{5.6}$$

as can be derived by substituting (2.6) in (5.1) and rescaling velocities.

For freely evolving and driven inelastic hard sphere fluids the scaling solutions $f(c)$ have been extensively discussed both in the bulk of the thermal distribution, as well as in the high energy tails [17, 12, 37, 19].

6 Scaling in d-dimensional free cooling

6.1 Fourier transform method

To determine scaling solutions for free cooling $(D = 0)$, we first consider the Fourier transform of the distribution function, $\Phi(k,t) = \langle \exp[-i\boldsymbol{k}\cdot\boldsymbol{v}]\rangle$, which is the characteristic or generating function of the velocity moments $\langle v^n \rangle$, and derive its equation of motion. Because $F(v,t)$ is isotropic, $\Phi(k,t)$ is isotropic as well.

As an auxiliary step we first Fourier transform the gain term in (5.2), i.e.

$$\begin{aligned}
&\int d\boldsymbol{v} \exp[-i\boldsymbol{k}\cdot\boldsymbol{v}]\, I_{\text{gain}}(v|F) = \\
&\int_n \int d\boldsymbol{v}d\boldsymbol{w} \exp[-i\boldsymbol{k}\cdot\boldsymbol{v}^*]F(v,t)F(w,t) = \int_n \Phi(k\eta_+,t)\Phi(k\eta_-,t). \quad (6.1)
\end{aligned}$$

The transformation needed to obtain the first equality follows by changing the integration variables $(\boldsymbol{v},\boldsymbol{w}) \to (\boldsymbol{v}^{**},\boldsymbol{w}^{**})$ and using the relation $d\boldsymbol{v}d\boldsymbol{w} = \alpha d\boldsymbol{v}^{**}d\boldsymbol{w}^{**}$. Then we use (5.3) to write the exponent as $\boldsymbol{k}\cdot\boldsymbol{v}^* = \boldsymbol{k}_-\cdot\boldsymbol{v} + \boldsymbol{k}_+\cdot\boldsymbol{w}$, where

$$\begin{aligned}
\boldsymbol{k}_+ &= p(\boldsymbol{k}\cdot\boldsymbol{n})\boldsymbol{n} \qquad |\boldsymbol{k}_+| = kp|(\hat{\boldsymbol{k}}\cdot\boldsymbol{n})| = k\eta_+(\boldsymbol{n}) \\
\boldsymbol{k}_- &= \boldsymbol{k} - \boldsymbol{k}_+ \qquad |\boldsymbol{k}_-| = k\sqrt{1 - z(\hat{\boldsymbol{k}}\cdot\boldsymbol{n})^2} = k\eta_-(\boldsymbol{n}), \qquad (6.2)
\end{aligned}$$

with $p = 1 - q = \frac{1}{2}(1+\alpha)$ and $z = 1 - q^2$. In one dimension $\eta_+(\boldsymbol{n}) = p$ and $\eta_-(\boldsymbol{n}) = q$, and $\int_n$ can be replaced by unity. The Fourier transform of (5.2) then becomes the Boltzmann equation for the characteristic function,

$$\partial_t\Phi(k,t) = -\Phi(k,t) + \int_n \Phi(k\eta_+(\boldsymbol{n}),t)\Phi(k\eta_-(\boldsymbol{n}),t), \qquad (6.3)$$

where $\Phi(0,t) = 1$ because of the normalization of the distribution function, and the collision operator is a $(d-1)-$dimensional integral. In one-dimension this equation simplifies to (2.8).

Next we consider the moment equations. Because $F(v,t)$ is isotropic, only its even moments are non-vanishing. If we assume that all moments $\langle v^n\rangle$ are *finite*, then the moment expansion of the characteristic function takes the form,

$$\Phi(k,t) = {\sum_n}' \frac{(-ik)^n}{n!}\langle(\hat{\boldsymbol{k}}\cdot\boldsymbol{v})^n\rangle = {\sum_n}'(-ik)^n m_n(t), \qquad (6.4)$$

and $\Phi(k,t)$ is a regular function of $\boldsymbol{k}$ at the origin. In the equation above the prime indicates that n is even, and the moments $m_n(t)$ are defined as,

$$m_n(t) = \beta_n\langle v^n\rangle/n!, \qquad (6.5)$$

where $\beta_s = \int_n(\hat{\boldsymbol{k}}\cdot\hat{\mathbf{a}})^s$ for real s is an angular integral over $\boldsymbol{n}$, given by:

$$\beta_s = \frac{\int_0^{\pi/2} d\theta(\sin\theta)^{d-2}(\cos\theta)^s}{\int_0^{\pi/2} d\theta(\sin\theta)^{d-2}} = \frac{\Gamma(\frac{s+1}{2})\Gamma(\frac{d}{2})}{\Gamma(\frac{s+d}{2})\Gamma(\frac{1}{2})}. \qquad (6.6)$$

Moreover, the normalizations (2.4) give $m_0(t) = 1$ and $m_2(t) = \frac{1}{2}\beta_2\langle v^2\rangle = \frac{1}{4}v_0^2(t)$. By inserting the moment expansion (6.4) in the Fourier transformed Boltzmann equation (6.3), we obtain the equations of motion for the coupled set of moment equations by equating the coefficients of equal powers of k. The result is,

$$\dot{m}_n + \lambda_n m_n = \sum_{l=2}^{n-2} h\,(l, n-l)\ m_l\, m_{n-l} \quad (n > 2) \tag{6.7}$$

with coefficients,

$$\begin{aligned} h(l,s) &= \textstyle\int_n \eta_+^l(\boldsymbol{n})\eta_-^s(\boldsymbol{n}) \\ \lambda_s = 1 - h(s,0) - h(0,s) &= \textstyle\int_n [1 - \eta_+^s(\boldsymbol{n}) - \eta_-^s(\boldsymbol{n})], \end{aligned} \tag{6.8}$$

where all labels $\{n, l, s\}$ take *even* values only. For later use we calculate λ_2 explicitly with the help of (6.2) with the result $\lambda_2 = 2pq/d$.

To obtain a scaling solution of (6.3) we set $\Phi(k,t) = \phi(kv_0(t))$ where the r.m.s. velocity is obtained from (5.5) with $D = 0$, and reads $v_0(t) = v_0(0)\times \exp(-pqt/d) = v_0(0)\exp(-\frac{1}{2}t\lambda_2)$. This gives the *integral* equation for the scaling form $\phi\,(k)$,

$$-\tfrac{1}{2}\lambda_2 k \tfrac{d}{dk}\phi\,(k) + \phi\,(k) = \textstyle\int_n \phi\,(k\eta_+)\,\phi\,(k\eta_-)\,, \tag{6.9}$$

which reduces for $d = 1$ to,

$$-\tfrac{1}{2}\lambda_2 k \tfrac{d}{dk}\phi(k) + \phi(k) = \phi(pk)\phi(qk). \tag{6.10}$$

Here $\phi(k)$ is the generating function for the moments μ_n of the scaling form $f(c)$, i.e.

$$\begin{aligned} \phi(k) &= \sum_n{}' \frac{(-ik)^n}{n!}\beta_n\langle c^n\rangle \equiv \sum_n{}'(-ik)^n\mu_n \\ &\simeq 1 - \tfrac{1}{4}k^2 + k^4\mu_4 - k^6\mu_6 + \cdots, \end{aligned} \tag{6.11}$$

where n is even, $\mu_0 = 1$ and $\mu_2 = \frac{1}{2}\beta_2\langle c^2\rangle = 1/4$ on account of the normalizations (2.7) and $\beta_2 = 1/d$ as given in (6.6).

6.2 Small-k singularity of the characteristic function

In the previous section we have obtained the Boltzmann equation (6.3) for the characteristic function, the moment equations (6.7), and the integral equation (6.9) for the scaling form $\phi(k)$. These equations provide the starting point for explaining the MD-simulations of Baldassarri et al. for the freely cooling IMM in two dimensions, i.e. data collapse after a short transient time on a scaling form $f(c)$ with a power law tail. In the present section we derive the solution $f(c)$ with a power law tail, and in Section 7 we will study the approach to this scaling form.

The strategy to determine analytically a possible solution with a power law tail is by assuming that such solutions exist, then inserting the ansatz $f(c) \sim 1/c^{a+d}$ into the scaling equation (6.9), and determining the exponent a such that the ansatz is indeed an asymptotic solution. We proceed as follows. Suppose that $f(c) \sim 1/c^{a+d}$, then the moments μ_n of the scaling form $f(c)$ are convergent for $n < a$ and are divergent for $n > a$. As we are interested in physical solutions which can be *normalized*, and have a *finite energy*, a possible value of the power law exponent must obey $a > 2$.

The characteristic function is in fact a very suitable tool for investigating this problem. Suppose the moment μ_n with $n > a$ diverges, then the n-th derivative of the corresponding generating function also diverges at $k = 0$, i.e. $\phi(k)$ has a singularity at $k = 0$. Then a simple rescaling argument of the inverse Fourier transform shows that $\phi(k)$ has a dominant small-k singularity of the form $\phi(k) \sim |k|^a$, where $a \neq even$. On the other hand, when all moments are finite, the characteristic function $\phi(k)$ is *regular* at the origin, i.e. can be expanded in powers of k^2.

We first illustrate our analysis for the one-dimensional case. As the requirement of finite total energy imposes the lower bound $a > 2$ on the exponent, we make the ansatz, consistent with (6.11), that the dominant small-k singularity has the form,

$$\phi(k) = 1 - \tfrac{1}{4}k^2 + A\,|k|^a\,, \tag{6.12}$$

insert this in (6.10), and equate the coefficients of equal powers of k. This yields,

$$\tfrac{1}{2}a\lambda_2 = \lambda_a \quad \text{or} \quad apq = 1 - p^a - q^a. \tag{6.13}$$

The equation has two roots, $a = 2, 3$, of which $a = 3$ is the one larger than 2. Here A is left undetermined. Consequently the one-dimensional scaling solution has a power law tail, $f(c) \sim 1/c^4$, in agreement with the exact solution (2.10).

For general dimension we proceed in the same way as in the one-dimensional case. We insert the ansatz (6.12) into (6.9), and equate the coefficients of equal powers of k. This yields for the coefficient of k^2 the identity $2pq/d = \lambda_2$, and for the coefficient of k^a the transcendental equation,

$$\tfrac{1}{2}a\lambda_2 = \textstyle\int_n \left[1 - \eta_+^a - \eta_-^a\right] = \lambda_a. \tag{6.14}$$

The equation above obviously has the solution $a = 2$. We are however interested in the solution with $a > 2$. In the elastic limit ($\alpha \to 1$) the solution is simple. There $q \to 0$ and a diverges. The contributions of $\eta_\pm^a$ on the right hand side vanish because $\eta_\pm < 1$, and the exponent has the form,

$$a \simeq \frac{d}{pq} = \frac{4d}{1-\alpha^2}. \tag{6.15}$$

This result has qualitatively the same shape as the numerical solution of (6.14), shown in Figure 3 for $d = 2$. Moreover the simplified BGK-model of Section 4 predicts the same qualitative behavior for the exponent of the power law tail. For general values of α one needs to evaluate the integrals $h(a, 0)$ and $h(0, a)$, defined in (6.8).

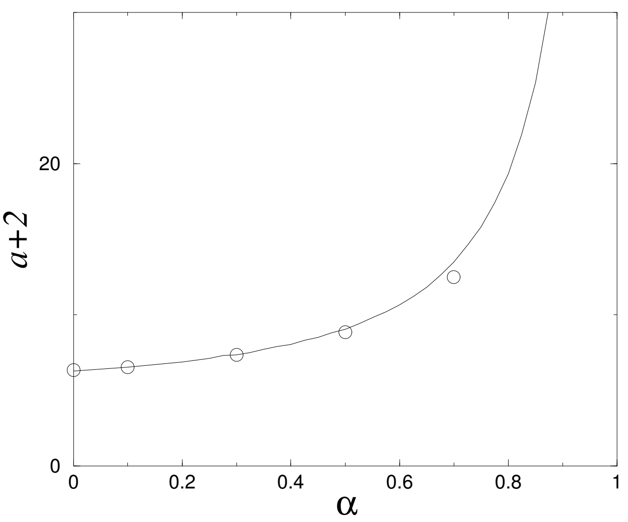

Figure 3: Exponent $a(\alpha)$ (solid line) as obtained by numerical solution of (6.14). The open circles represent the exponents, measured from the velocity distribution functions obtained from MC simulations, and shown in Fig. 5. Figure from Ref.[19].

Here we only quote the results, and refer for technical details to the literature [35, 31], i.e.

$$h\,(a, 0) = p^a \beta_a; \qquad h\,(0, a) = \,{}_2F_1\Big(-\tfrac{a}{2}, \tfrac{1}{2}; \tfrac{d}{2}; z\Big), \tag{6.16}$$

where β_a is given in (6.6), and ${}_2F_1$ is the hypergeometric function with $z = 1 - q^2$. One can conveniently use an integral representation of ${}_2F_1$ to solve this transcendental equation numerically. We illustrate the solution method of (6.14) with the graphical construction in Figure 4, where we look for intersections of the line $y = \frac{1}{2}s\lambda_2 = \gamma_0 s$ with the curve $y = \lambda_s$ for different values of α.

The relevant properties of λ_s are: (i) $\lim_{s\to 0} \lambda_s = -1$ whereas $\lambda_0 = 0$ because of particle conservation; (ii) λ_s is a concave function, monotonically increasing with s, and *(iii)* all eigenvalues for positive *integers* n are positive (see Figure 4). As can be seen from the graphical construction, the transcendental equation (6.14) has two solutions, the trivial one $(s_0 = 2)$ and the solution $s_1 = a$ with $a > 2$.

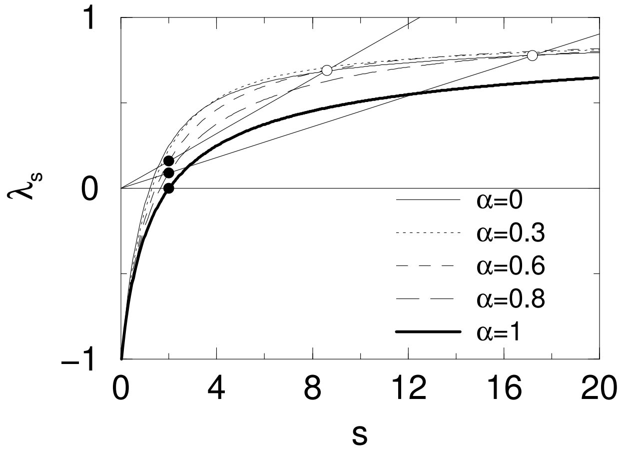

Figure 4: Graphical solution of (6.14) for different values of the paramenter α. The eigenvalue λ_s is a concave function of s, plotted for different values of the restitution coefficient α for the 2-D inelastic Maxwell model. The line $y = s\gamma_0 = \frac{1}{2}s\lambda_2$ is plotted for $\alpha = 0.6, 0.8$ and $\alpha = 1$(top to bottom). The intersections with λ_s determine the points s_0 (filled circles) and s_1 (open circles). Here $s_1 = a$ determines the exponent of the power law tail. For the elastic case ($\alpha = 1, q = 0$) there is only one intersection point.

The numerical solutions $s_1(\alpha)$ for $d = 2$ are shown in Figure 3 as a function of α, and the α-dependence of the root $a(\alpha)$ can be understood from the graphical construction. In the elastic limit as $\alpha \uparrow 1$ the eigenvalue $\lambda_2(\alpha) \to 0$ because of energy conservation. In that limit the transcendental equation (6.14) no longer has a solution with $a > 2$, and $a(\alpha) \to \infty$ according to (6.15), as it should be. This is consistent with a Maxwellian tail distribution in the elastic case. Krapivsky and Ben-Naim [31] have also solved the transcendental equation asymptotically for large d ($d \gg 1$), which gives qualitatively the same results as those shown in Figure 3 for two dimensions.

These results establish the existence of scaling solutions $f(c) \sim 1/c^{d+a}$ with algebraic tails, where the exponent a is the solution of the transcendental equation (6.14). Using a somewhat different analysis Krapivsky and Ben-Naim [31] obtained the same results for the algebraic tails in freely cooling Maxwell models.

The previous results have been confirmed in a quantitative manner by means of MC simulations in [30, 19] for different values of α. The algebraic tails of $f(c)$ are shown in Fig. 5, and the exponents a, measured from the MC data in Figure 5 are plotted in Fig. 3. Both graphs show excellent agreement with the analytic results, derived here.

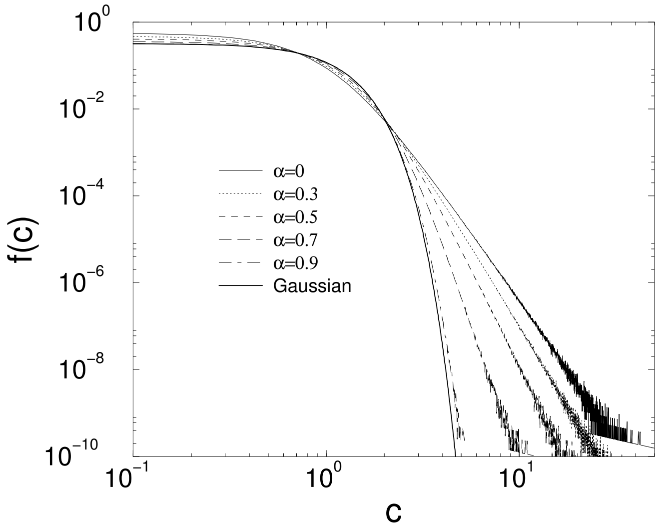

Figure 5: Simulation of the velocity distribution function by the MC method, showing power law tails. Figure from Ref. [19].

7 Moment equations and approach to scaling

7.1 Moments of velocity distributions

In this section we study the effects on the moments of power law tails in the scaling form, and we analyze in what sense the *even* moments $m_n(t) = \beta_n \langle v^n \rangle / n!$ at large times are related to the moments $\mu_n = \beta_n \langle c^n \rangle / n!$ of the scaling form $f(c) \sim 1/c^{a+d}$, which are *divergent* for $n > a$ and remain *finite* for $n < a$.

First consider the moment equations (6.7) where $m_0(t) = 1$ and $m_2(t) = m_2(0) \exp[-\lambda_2 t] = \frac{1}{4} v_0^2(t)$. Similarly one shows [35, 31] that $m_n(t) \sim \exp[-\lambda_n t]$ for large t. Consequently all moments with $n > 0$ vanish as $t \to \infty$, consistent with the fact $F(v,t) \to \delta^{(d)}(\boldsymbol{v})$ in this limit.

The rescaled moments $\mu_n(t) \equiv m_n(t)/v_0^n(t)$ show a more interesting behavior. We analyze how they approach their limiting form $\mu_n(\infty)$. Inserting this definition into the moment equations (6.7) and using $v_0(t) = v_0(0) \exp[-\frac{1}{2}\lambda_2 t]$ we find for the rescaled even moments with $n > 0$,

$$\begin{aligned} \dot{\mu}_n(t) + \gamma_n \mu_n(t) &= \sum_{l=2}^{n-2} h(l, n-l) \mu_l(t) \mu_{n-l}(t) \\ \gamma_n &= \lambda_n - \tfrac{1}{2} n \lambda_2. \end{aligned} \tag{7.1}$$

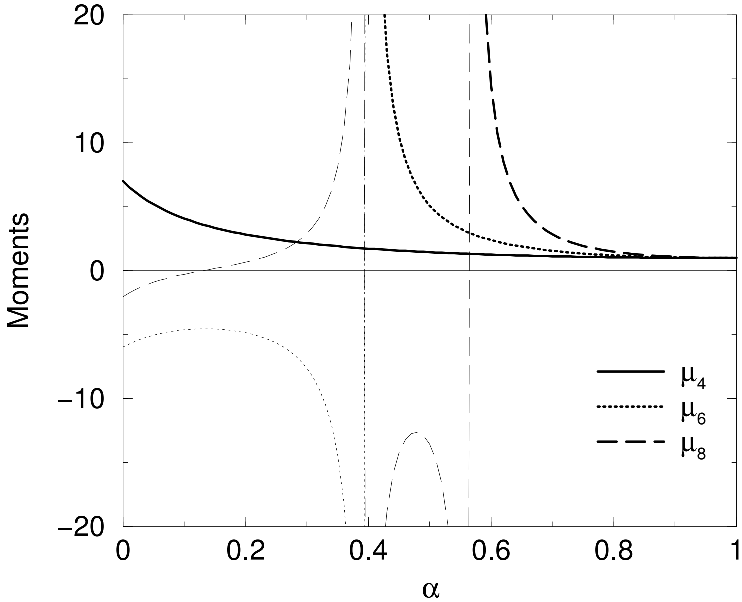

Figure 6: Moments μ_4, μ_6 and μ_8 as a function of the coefficient of restitution α. Starting at $\alpha = 1$ the moment μ_n increases monotonically as α decreases following the physical branch (thick line) untill α reaches a zero of γ_s, where μ_n diverges towards $+\infty$. The recursion relation (7.3) has a second set of solutions $\{\mu_n\}$ that become negative for small α, indicating unphysical solutions.

The infinite set of moment equations (7.1) for $\mu_n(t)$ can be solved sequentially for all n as an initial value problem. To explain what is happening, it is instructive to consider again the graphical solution of the equation, $\gamma_s = \lambda_s - \frac{1}{2}s\lambda_2 = 0$ for different values of the inelasticity q or α, as illustrated by the intersections $\{s_0, s_1\}$ of the curve $y = \lambda_s$ and the line $y = \frac{1}{2}s\lambda_2$, where s_0 and s_1 are denoted respectively by filled ($\bullet$) and open circles ($\circ$). These circles divide the spectrum into a *stable* branch ($s_0 < s < s_1$) and two *unstable* branches ($s < s_0$) and ($s > s_1$). The moments $\mu_s(t)$ with $s = n > a$ are on an unstable branch ($\gamma_s < 0$) and will grow for large t at an exponential rate, $\mu_n(t) \simeq \mu_n(0)\exp[|\gamma_n|t]$, as can be shown by complete induction from (7.1) starting at $n = [a] + 1$. They remain positive and finite for finite time t, but approach $+\infty$ as $t \to \infty$, in agreement with the predictions of the self consistent method of Section 6. The moments μ_n with $n = 2, 4, \cdots, [a]$ with n on the stable branch are globally stable and approach for $t \to \infty$ the limiting value $\mu_n(\infty) = \mu_n$, which are the finite positive moments of the scaling form (7.2), plotted in Fig. 6. In summary, $\mu_n(t) \to \infty$ if $n > a$, and $\mu_n(t)$ approach $\mu_n(\infty) = \mu_n$ for $n < a$, in agreement with the predictions of the power law tails in Section 6.2.

The behavior of the moments described above is considered as a weak form of convergence or approach of the distribution function $F(v,t)$ to the scaling form $f(c)$ for $t \to \infty$. The physically most relevant distribution functions are those with *regular* initial conditions, i.e. all moments $m_n(0) = v_0^n(0)\mu_n(0) < \infty$.

7.2 Moments of scaling forms

Next we consider the moments μ_n generated by the scaling form $\phi(k)$ in (6.12), corresponding to $f(c) \sim 1/c^{a+d}$, where $a > 2$ and not equal to an even integer. This implies that the $n-$th order derivatives of $\phi(k)$ at $k = 0$, and equivalently all moments μ_n, are *finite* if $n \leq [a] < a$, and all those with $n > a$ are *divergent*. Here $[a]$ is the largest integer less than a where $[a]$ may be an even or odd integer. Hence, the *small-k* behavior of $\phi(k)$ can be represented as ,

$$\phi(k) = \sum_{n=0}^{[a]}{}'(-k)^n \frac{\mu_n}{n!} + o(|k|^a), \tag{7.2}$$

where the prime on the summation sign indicates that n takes only even values. The remainder is of order $o(|k|^a)$ as $k \to 0$. In this finite sum we only know the exponent a and the moments $\mu_0 = 1$ and $\mu_2 = 1/4$. Now we calculate the unknown finite moments of the scaling form, μ_n with $2 < n \leq [a]$. This is done by insert ing (7.2) into the kinetic equation (6.9), yielding the recursion relation,

$$\mu_n = (1/\gamma_n) \sum_{l=2}^{n-2} h(l, n-l)\mu_l \mu_{n-l} \tag{7.3}$$

with initialization $\mu_2 = 1/4$, where l and n are even. The solutions μ_n for $n = 4, 6, 8$ are shown in Fig. 6 as a function of the coefficient of restitution α. The physical branches of these functions are the ones that start positive at $\alpha = 1$. Furthermore we observe that the root $s = a$ of the transcendental equation (6.14), $\gamma_s = \lambda_s - \frac{1}{2}s\lambda_2 = 0$, indicates that γ_s changes sign at $s_1 = a$ (see open circles in Fig.4). This change of sign, where the branch becomes unphysical, can according to Section 6 be interpreted as all moments μ_n with $n > s_1 = a$ (n on unstable branch) becoming *divergent*. That this interpretation is the correct one, has already been demonstrated in the Section 7.1, where it is shown that for $n > a$ the reduced moments $\mu_n(t) \to \infty$ as $t \to \infty$.

The recursion relation (7.3) for the moments μ_n in the one-dimensional case is again a bit pathological in the sense that the *stable* branch $(s_0 = 2 < s \leq s_1 = 3)$

contains only one single integer label, i.e. $s = 3$. So only $\mu_0 = 1$ and $\mu_2 = 1/4$ are finite, and all other moments are infinite, in agreement with the exact solution of Baldassarri et al.

The recursion relation (7.3) has a *second* set of solutions $\{\mu_n\}$, simply defined by iterating the recursion relation for n arbitrary large. This set contains *negative* moments μ_n [26]. The argument is simple. Consider μ_n in (7.3) with $n = [a] + 1$. Then the pre-factor $1/\gamma_{[a]+1}$ on the right hand side of this equation is negative because the label $[a] + 1 > a$ is on the unstable branch of the eigenvalue spectrum in Fig.4, while all other factors are positive. This implies that the corresponding scaling form $f(c)$ has negative parts, and is therefore physically not acceptable. We also note that the moments μ_n of the physical and the unphysical scaling solution $\phi(k)$ coincide as long as both are *finite* and *positive* in the $\alpha-$interval that includes $\alpha = 1$. These unphysical solutions are also shown in Fig.6.

8 Driving and non-equilibrium steady states

8.1 Energy balance

The present section is devoted to the study of systems of inelastic Maxwell particles with energy input. Here the system may or may not be able to reach a non-equilibrium steady state (NESS). To reach a spatially homogeneous steady state, energy has to be supplied homogeneously in space. This may be done by applying an external stochastic force to the particles in the system, or by connecting the system to a thermostat, modelled by a frictional force with *negative* friction. Complex fluids (e.g. granular) subject to such forces can be described by the microscopic equations of motion for the particles, $\dot{\boldsymbol{r}}_i = \boldsymbol{v}_i$, and $\dot{\boldsymbol{v}}_i = \boldsymbol{a}_i + \tilde{\xi}_i$ $(i = 1, 2, \cdots)$, where $\boldsymbol{a}_i$ and $\tilde{\xi}_i$ are the possible friction and random forces respectively. If needed one may also include in $\boldsymbol{a}_i$ a conservative (velocity independent) force.

Regarding the Negative Friction (NF) thermostats, the most important and most common choice [18] is a friction, linear in the velocity, $+\gamma \boldsymbol{v}$, the so-called *iso-kinetic* or *Gaussian thermostat* [45, 46]. A second example of a negative friction force is $\boldsymbol{a} = \zeta \hat{\boldsymbol{v}}$, which is acting in the direction of the particle's velocity, but independent of its speed. Furthermore, the external stochastic force, $\tilde{\xi}_i$, is taken to be Gaussian white noise with zero mean, and variance,

$$\overline{\tilde{\xi}_{i,\alpha}(t)\tilde{\xi}_{j,\beta}(t')} = 2D\delta_{ij}\delta_{\alpha\beta}\delta(t-t'), \tag{8.1}$$

where α, β denote Cartesian components, and D is the noise strength. The Boltzmann equation, describing a spatially homogeneous system driven in this manner, takes the form,

$$\partial_t F(v) + (\boldsymbol{\nabla}_v \cdot \boldsymbol{a} - D\nabla_v^2)F(v) = I(v|F), \tag{8.2}$$

where $\mathcal{F} = \boldsymbol{\nabla}_v \cdot \boldsymbol{a} - D\nabla_v^2$ represents the driving term.

Next we consider the *balance equation* for the granular temperature in driven cases, where the external input of energy counterbalances the collisional cooling, and may lead to a NESS. We proceed in the same manner as for the free case, and apply $(\int d\boldsymbol{v}v^2)$ to the Boltzmann equation in (8.2) with the result,

$$d\langle v^2\rangle/dt = \int d\boldsymbol{v}\, v^2 I(v|F) + 2\langle \boldsymbol{v}\cdot\boldsymbol{a}\rangle + 2dD. \tag{8.3}$$

The second and third term are obtained from the driving term in (8.2) by performing partial integrations. The most common way of driving dissipative fluids in theoretical and MD studies [12, 18, 31, 27, 47, 48] is by Gaussian white noise (WN) $(\boldsymbol{a} = 0; D \neq 0)$. We include in our studies also the two types of NF-thermostat $(\boldsymbol{a} \neq 0; D = 0)$, discussed above. The resulting energy balance equation is,

$$\frac{dv_0}{dt} = \begin{cases} \frac{2D}{v_0} - \frac{pq}{d}v_0 & \text{(WN)} \\ \frac{2\zeta\langle|c|\rangle}{d} - \frac{pq}{d}v_0 & \text{(const NF)} \\ (\gamma - \frac{pq}{d})v_0 & \text{(iso-kin)} \end{cases} \tag{8.4}$$

Here we have used the relation, $\langle|v|\rangle = v_0\langle|c|\rangle$, where the last average $\langle|c|\rangle$ is a moment of $f(c)$. One sees that the collisional loss is counterbalanced by the heat, generated by randomly kicking the particles or by the negative friction of the Gaussian thermostat.

The stationary solutions of the first two equations are stable attractive fixed points, which are approached at an exponential rate,

$$v_0(\infty) = \begin{cases} \sqrt{2dD/pq} & \text{(WN)} \\ \frac{2\zeta\langle|c|\rangle}{pq} & \text{(const NF)} \end{cases} \tag{8.5}$$

The case of driving by an iso-kinetic thermostat (with *linear* negative friction) is a marginal case, discussed in [19], because stationarity is only reached when the friction constant has exactly the value $\gamma = pq/d$, in which case any initial value $v_0(0)$ is stationary. So, for an inelastic Maxwell gas, driven by an iso-kinetic thermostat, there does *not exist* a stationary state, because the general solution of the rate equation for arbitrary value of γ is,

$$v_0(t) = v_0(0)\exp[(\gamma - pq/d)t] \qquad \text{(iso-kin)}, \tag{8.6}$$

which may be increasing or decreasing as $t \to \infty$, depending on the inequalities, $\gamma < \gamma_0$ or $\gamma > \gamma_0$.

8.2 Scaling equation

The equations (8.2) and (8.5) show that the NESS solution $F(v,\infty)$ depends strongly on the mode of energy supply. To exhibit possible universal features of the solution we measure velocities in their typical magnitude, i.e. the r.m.s. velocity $v_0(\infty)$, just like in thermal equilibrium, and introduce the rescaled distribution,

$$F(v,\infty) = \frac{1}{v_0^d(\infty)} f\left(\frac{v}{v_0(\infty)}\right). \tag{8.7}$$

The integral equation for the scaling form $f(c)$ follows in this case by inserting (8.7) in (8.2), and setting $\partial_t F = 0$, i.e.

$$I(c|f) = \begin{cases} -\dfrac{D}{v_0^2(\infty)}\nabla_c^2 f & = -\dfrac{pq}{2d}\nabla_c^2 f \qquad \text{(WN)} \\ \dfrac{\zeta}{v_0(\infty)}\boldsymbol{\nabla}_c\cdot(\hat{\boldsymbol{c}}f) & = \dfrac{pq}{2d\,\langle|c|\rangle}\boldsymbol{\nabla}_c\cdot(\hat{\boldsymbol{c}}f) \qquad \text{(const NF)} \end{cases} \tag{8.8}$$

In the second equality on both lines $v_0(\infty)$ has been eliminated with the help of (8.5).

Next we consider the special case of a system driven by an iso-kinetic thermostat ($\boldsymbol{a} = \gamma\boldsymbol{v}; D = 0$), where $F(v,t)$ does not approach a NESS, but rapidly reaches a scaling state, described by (2.6) and having the time dependent r.m.s. $v_0(t)$ in (8.6). In that case the terms $\partial_t F$ and $\mathcal{F}F$ in Eq. (8.2) produce respectively the terms $(-\gamma + pq/d)\ \boldsymbol{\nabla}_c\cdot(\boldsymbol{c}f)$ and $\gamma\boldsymbol{\nabla}_c\cdot(\boldsymbol{c}f)$. So the terms containing the friction constant γ cancel. The scaling equation for the iso-kinetic thermostat then becomes,

$$I(c|f) = \frac{pq}{d}\boldsymbol{\nabla}_c\cdot(\boldsymbol{c}f) \qquad \text{(iso-kin)}. \tag{8.9}$$

This scaling equation is *identical* to the one derived in (5.6) for free cooling, and no trace of the friction constant γ of the iso-kinetic thermostat remains. For the case of inelastic hard spheres the equivalence of the integral equations for the scaling form in both cases has been observed before by Montanero and Santos [18]. However the big difference between inelastic Maxwell particles and inelastic hard spheres is that the latter system has an energy balance equation with a stable attracting fixed point solution, but a NESS does not exist in the former case.

8.3 High energy tails

The scaling equations for inelastic Maxwell particles [36] in the previous subsection cannot be solved exactly. However its asymptotic solution for $c \gg 1$ can be determined by the same procedure as used for inelastic hard spheres [12]. To do so we neglect the gain term in $I(c|f)$ in (8.8). Then $I(c|f)$ is replaced by $I_{\text{loss}}(c|f) \sim -f(c)$, and the asymptotic solutions of (8.8) are found in the form of stretched Gaussians, $f(c) \sim \exp[-\beta c^b]$ with positive b and β. One then verifies *a posteriori* that the stretched Gaussians are indeed consistent solutions of (8.8) and (8.9) by substitution them back into $I(c|f)$, and showing [36] that the loss term is asymptotically dominant over the gain term as long as exponent b and coefficient β are positive.

After these preparations we insert the stretched exponential form into the Boltzmann equation (8.8), and match the leading exponents on both sides of the equation, as well as the coefficients in the exponents of these terms. This gives the following results for the asymptotic high energy tail, $f(c) \sim \exp[-\beta c^b]$, in $d-$dimensional inelastic Maxwell models,

$$\begin{array}{lll} b=1 & \beta=\sqrt{\frac{2d}{pq}} & \text{(WN)} \\ b=1 & \beta=\frac{2d\langle|c|\rangle}{pq} & \text{(const NF)} \\ b=0 & \text{inconsistent} & \text{(iso-kin).} \end{array} \tag{8.10}$$

We conclude this subsection about driven inelastic Maxwell models with some comments:

Why is the result, $b = 0$, inconsistent for the *iso-kinetic* thermostat in this model? Taking the limit $b \to 0$ in $\exp[-\beta c^b]$ suggests that $f(c)$ has indeed a power law tail. As we have seen in (8.9), the scaling equation for the IMM driven by this thermostat is equivalent with the scaling equation for free cooling, and we know from the analysis in Section 6.2 that $f(c) \sim 1/c^{a+d}$ has indeed a power law tail. However the exponent a that would have been obtained from (8.9) with I replaced by $I_{\text{loss}} \sim -f(c)$ does not yield a consistent solution. In the limit $b \to 0$ the gain term I_{gain} can no longer be neglected with respect to the loss term. That this is indeed the case can be seen from (6.14), where the terms η_+^a and η_-^a originate from the gain term. These terms give substantial contributions to the value of a, and are even dominant for small values of α. We also note that in the case of driving by an iso-kinetic thermostat—which turns out to be equivalent to the free cooling IMM system—the driven system does not reach a nonequilibrium steady state, but keeps either heating up or cooling down, depending on the thermostat strength γ.

White noise driving and positive b lead for all $d \geq 1$ to consistent asymptotic solutions of the scaling equations with overpopulated high energy tails of simple exponential type, $f(c) \sim \exp[-c\sqrt{2d/pq}]$ (Refs.[36, 38]), in complete agreement with the asymptotic result (3.6), and in qualitative agreement with the corresponding result (4.5) for BGK-models. Here *all* moments $\int dc c^n f(c) < \infty$. This would not be the case for power law tails. The one-dimensional version of this problem has been extensively studied by Nienhuis and van der Hart [42], and by Antal et al. [44] using MC simulations of the Boltzmann equation. MC simulations of the two-dimensional version of this problem have been carried out in Ref. [19].

When the IMM system is driven by a *constant NF*-thermostat the scaling function also shows an exponential tail, $f(c) \sim \exp[-2d\langle c\rangle c/pq]$, with a coefficient that depends on the first moment $\langle c\rangle$ of the complete scaling $f(c)$. In Refs. [12, 37, 19] methods have been developed to calculate these moments perturbatively.

For comparison we also quote the high energy tail for $d-$dimensional inelastic hard spheres, which are also of the form of stretched Gaussians, and we quote the results for the exponents b and the coefficients β for the different modes of energy supply, i.e.

$$\begin{array}{lll} b=3/2 & \beta=\sqrt{\frac{2d\beta_1}{pq\kappa_3}} & \text{(WN)} \\ b=2 & \beta=\frac{\beta_1\langle|c|\rangle}{pq\kappa_3}\simeq\frac{1}{\sqrt{2}pq} & \text{(const NF)} \\ b=1 & \frac{d\beta_1}{pq\kappa_3} & \text{(iso-kin)} \end{array} \tag{8.11}$$

where β_1 is given in (6.6), $\langle c\rangle = \int d\boldsymbol{c} c f(c)$ and $\kappa_3 = \int_n \int d\boldsymbol{c} d\boldsymbol{u} |(\boldsymbol{c}-\boldsymbol{u})\cdot\boldsymbol{n}|^3 f(c) f(u)$ [37]. For α close to unity the replacement of $f(c)$ by the Gaussian $\pi^{-d/2}\exp[-c^2]$ gives a good approximation, yielding $\langle c\rangle \simeq 1/[\sqrt{\pi}\beta_1]$ and $\kappa_3 = \sqrt{2/\pi}$. The results for the WN- and iso-kinetic thermostat have been first derived in [12], and confirmed by MC simulations in [18]. The theoretical result for the *constant* NF thermostat was first derived in [18], but its consistency was questioned. For that reason we have verified the consistency of the result (8.11) a posteriori, and we confirm that it is indeed an asymptotic solution of (8.8) with the full Boltzmann collision operator, as long as $\alpha < 1$.

9 Conclusions

In the present paper we have reviewed the new developments on anomalous velocity distributions in gases of inelastic Maxwell models (IMM), and compared the results with those for the proto-typical granular model, the inelastic hard spheres (IHS). The velocity distributions, obtained in this article, are scaling or similarity solutions (2.6) of the nonlinear Boltzmann equation.

The dominant common feature in all these results is that the inelasticity of the collisions creates *over-populations* of high energy tails of the velocity distribution $F(v,t)$, when compared to the Gaussian Maxwell-Boltzmann distribution $F(v,\infty)$ in thermal equilibrium of systems of elastic particles. At finite inelasticity $(\alpha < 1)$ the overpopulations in the high energy tails are power laws, $f(c) \sim 1/c^{a+d}$ (free cooling in IMM), or stretched Gaussians, $\exp[-\beta c^b]$ with $0 < b < 2$ (free cooling IHS and driven IMM and IHS).

An intermezzo, presented in Section 4, shows that the results obtained for inelastic Maxwell models are rather robust. We consider an extremely simplified inelastic BGK-model, and show that the resulting over-populations of high energy tails, both with and without energy input, are qualitatively the same as for the nonlinear Boltzmann equation of inelastic Maxwell models in $d-$dimensions.

Returning to the main menu of IMM's, we note that the degree of overpopulation is decreasing ($b \uparrow 2$) with the increasing efficiency to randomize the velocities of the highly energetic particles, either by collisions or by the external forcing terms. As the IHS's have a larger collision frequency, $\propto g$, than the IMM's with a constant collision frequency, the IHS have smaller over-populations than the IMM's. Because external white noise applied to freely cooling inelastic gases adds an extra mechanism for randomization, the tails in the driven cases show lower over-populations than in the freely cooling case.

A intriguing question about over-populated tails: "Are power laws or stretched exponentials the generic form of over-populated tails in inelastic models", is difficult to answer because we have only information from two different interaction models. In two very recent articles [37, 19] new classes of inelastic models have been introduced, that correspond to soft spheres with repulsive interactions $(1/r^s)$. These soft spheres have a collision frequency $\propto g^\nu$ with $\nu = 1 - 2(d-1)/s$. The limit $s \to \infty$, or $\nu \uparrow 1$, corresponds to strong IHS interactions at high energy. In the limit $\nu \downarrow 0$, analogously to $s \downarrow 2(d-1)$, the interactions decrease. For $\nu \geq 0$ the IMM-interactions $(\nu = 0)$ are the weakest of all. The results for these inelastic soft spheres models [37, 19], corresponding to (8.10) and (8.11), are again stretched Gaussians $f(c) \sim \exp[-\beta c^b]$ with

$$\begin{aligned} b &= \tfrac{1}{2}(\nu + 2) \qquad && (\text{WN; } \nu \geq 0) \\ b &= \nu && (\text{iso-kin; } \nu > 0\ ) \end{aligned} \tag{9.1}$$

The limit $b = \nu \downarrow 0$ for the iso-kinetic thermostat, which also corresponds to free cooling (see Section 8), is consistent with a power law tail. This analysis shows that the generic type of over-population is a stretched Gaussian. A freely cooling IMM with $f(c) \sim 1/c^{a+d}$ is an isolated borderline case, that is most likely not the best model to describe the short range, hard core impulsive interactions of granular particles.

At the end of Section 3 we have seen in Table I the phenomenon of compressed Gaussians with $b > 2$, corresponding to under-population of high energy tails. The solutions with two delta peaks are extreme cases of compressed Gaussians. More extensive discussions of compressed Gaussians and of peak-splitting in one-dimensional inelastic models can be found in [15, 43, 19].

Acknowledgements

The authors want to thank J.W. Dufty, A. Santos, E. Trizac, A. Barrat and K. Shundyak for helpful discussions and correspondence. This work is supported by DGES (Spain), Grant No BFM-2001-0291.

References

[1] H.H. Jaeger, S.R. Nagel and R.P. Behringer, Rev. Mod. Phys., **68**, 1259 (1996).

[2] J.T. Jenkins and M.W. Richman, Phys. Fluids, **28**, 3485 (1985).

[3] N. Sela and I. Goldhirsch, Phys. Fluids, **7**, 507 (1995), and I. Goldhirsch, Chaos **9**, 659 (1999).

[4] T. Pöschel and S. Luding (eds.), *Granular Gases*, Lecture Notes in Physics, Vol. 564 (Springer, Berlin, 2000).

[5] T. Pöschel and N.V. Brilliantov (eds.), *Granular Gas Dynamics*, Lecture Notes in Physics, Vol. 624 (Springer, Berlin, 2003).

[6] C.S. Campbell, Annu. Rev. Fluid Mech., **22**, 57 (1990).

[7] I. Goldhirsch and G. Zanetti, Phys. Rev. Lett., **70**, 1619 (1993); I. Goldhirsch, M.L. Tan and G. Zanetti, J. Scientific Computing **8**, 1 (1993).

[8] S. McNamara and W.R. Young, Phys. Rev. E, **50**, R28 (1994).

[9] Y. Du, H. Li and L.P. Kadanoff, Phys. Rev. Lett., **74**, 1268 (1995).

[10] F. Melo, P.B. Umbanhowar and H.L. Swinney, Phys. Rev. Lett. **75**, 3838 (1995), and C. Bizon, M.D. Shattuck, J.B. Swift, and H.L. Swinney, Phys. Rev. E, **6**, 4340 (1999).

[11] S.E. Esipov and J. Pöschel, J. Stat. Phys., **86**,1385 (1997).

[12] T.P.C. van Noije and M.H. Ernst, Granular Matter, **1**, 57 (1998) and cond-mat/980342.

[13] G. P. Collins, Sci. Am., **284**(1), 17 (2001); F. Rouyer and N. Menon, Phys. Rev. Lett., **85**, 3676 (2000); J.S. Olafsen and J.S. Urbach, Phys. Rev. E, **60**, R2468 (1999); W. Losert, D.G.W. Cooper, J. Delour, A. Kudrolli, abd J.P. Gollub, Chaos, **9**, 682 (1999).

[14] I. Pagonabarraga, E. Trizac, T.P.C. van Noije and M.H. Ernst, Phys. Rev. E, **65**, 011303 (2002).

[15] A. Barrat, T. Biben, Z. Rácz, E. Trizac, and F. van Wijland, J. Phys. A: Math. Gen., **35**, 463 (2002) and cond-mat/0110345.

[16] D. Benedetto, E. Caglioti, J.A. Carrillo and M. Pulvirenti, J. Stat. Phys. **91**, 979 (1998).

[17] J.J. Brey, M.J. Ruiz-Montero, and D. Cubero, Phys. Rev. E, **54**, 3664 (1996) and **61**, 5573 (2000).

[18] J.M. Montanero and A. Santos, Granular Matter, **2**, 53 (2000), and cond-mat/0002323.

[19] M.H. Ernst, E. Trizac and A. Barrat, preprint.

[20] J.W. Dufty, in *Advances in Complex Systems*, edited by A. Mehta and T.C. Halsey **4**, No.4 (World Scientific, 2001), pp 397-406, and cond-mat/0108444.

[21] J.J. Brey, J.W. Dufty and A. Santos, J. Stat. Phys., **87**, 1051 (1997).

[22] D.R.M. Williams and F.C. MacKintosh, Phys. Rev. E, **54**, R9 (1996).

[23] A.V. Bobylev, Sov. Phys. Dokl. **20**, 820 (1976); M. Krook and T.T. Wu, Phys. Rev. Lett. **36**, 1107 (1976); M.H. Ernst, Phys. Rep. **78**, 1 (1981).

[24] J.J. Brey, F. Moreno, J.W. Dufty, Phys. Rev. E **54**, 445 (1996).

[25] E. Ben-Naim and P.L. Krapivsky, Phys. Rev. E, **61**, R5 (2000).

[26] A.V. Bobylev, J.A. Carrillo, and I.M. Gamba, J. Stat. Phys., **98**, 743 (2000); see also erratum: J. Stat. Phys., **103**, 1137 (2001).

[27] J.A. Carrillo, C. Cercignani, and I.M. Gamba, Phys. Rev. E, **62**, 7700 (2000)

[28] A. Baldassarri, U. Marini Bettolo Marconi, and A. Puglisi, Europhys. Lett., **58**, 14 (2002).

[29] A. Baldassarri, U. Marini Bettolo Marconi, and A. Puglisi, Phys. Rev. E, **65**, 051301 (2002).

[30] A. Baldassarri, U. Marini Bettolo Marconi and A. Puglisi, in Ref.[5].

[31] P.L. Krapivsky and E. Ben-Naim, J. Phys. A: Math Gen., **35**, L147 (2002), and cond-mat/0111044.

[32] E. Ben-Naim and P.L. Krapivsky, Phys. Rev. E, **66**, 11309 (2002), and cond-mat/0202332.

[33] E. Ben-Naim and P.L. Krapivsky, in Ref.[5] and cond-mat/0301238.

[34] M.H. Ernst and R. Brito, Europhys. Lett., **58**, 182 (2002) and cond-mat/0111093.

[35] M.H. Ernst and R. Brito, J. Stat. Phys., **109**, 407 (2002) and cond-mat/0112417.

[36] M.H. Ernst and R. Brito, Phys. Rev. E, **65**, 040301(R) (2002).

[37] M.H. Ernst and R. Brito, in Ref.[5], and cond-mat/0304608.

[38] A.V. Bobylev and C. Cercignani, J. Stat. Phys., **106**, 547 (2002).

[39] A.V. Bobylev, C. Cercignani and G. Toscani, J. Stat. Phys., **111**, 403 (2003).

[40] I.M. Gamba, V. Panferov and C. Villani, math.AP/0302348.

[41] A.V. Bobylev, I.M. Gamba and V. Panferov, math-ph/0306014.

[42] B. Nienhuis and R. van der Hart, unpublished; R. van der Hart, *Road Models and Granular Gases*, Master's thesis, Universiteit van Amsterdam, May 24, 2002.

[43] A. Santos and M.H. Ernst, Phys. Rev. E, **68**, 011305 (2003).

[44] T. Antal, M. Droz, and A. Lipowski, Phys. Rev. E, **66**, 062301 (2002), and cond-mat/0207102.

[45] D. Evans and G.P. Morriss, *Statistical mechanics of nonequilibrium liquids* (Academic Press, London, 1990).

[46] N.I. Chernov, G.I. Eyink, J.L. Lebowitz, and Ya. G. Sinai, Comm. Math. Physics, **154**, 569 (1993).

[47] T.P.C.van Noije, M.H.Ernst, E.Trizac and I. Pagonabarraga, Phys. Rev. E, **59**, 4326 (1999).

[48] G. Peng and T. Ohta, Phys. Rev. E, **58**, 4737 (1998).